

Figure 1.1: Row- and column sums of absorptions for a 3×3 object.

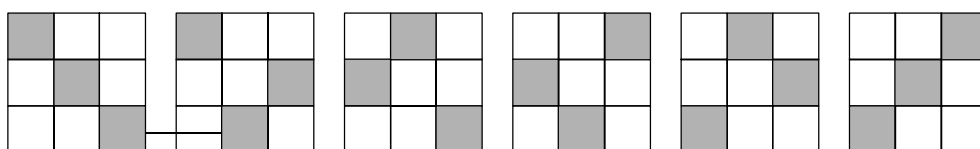


Figure 1.2: Six 3×3 sample objects with the same row- and column sums.

1.4 Least Squares Approach

To understand the idea behind the back projection method (how to achieve the reconstruction, how much data is needed etc.) we consider first a very small object - a 3×3 structure of 9 homogeneous blocks. Assuming first that the block densities are either 0 or 1, Figure 1.1 shows how the absorptions (sums over the blocks) add up along rows and columns. In this simple case, the data is easily seen to be sufficient for an exact inversion (since a row- or column sum of 3 settles all the elements in that row/column). However, had all row- and column sums added up to 1, Figure 1.2 shows that there would be six possible solutions (corresponding to the entries of the six different 3×3 permutation matrices). Even when the densities are limited to be either 0 or 1, row- and column sums give in general insufficient information for a reconstruction.

In realistic applications, the density of a block is a continuous variable. We next allow arbitrary densities of the blocks

x_1	x_4	x_7
x_2	x_5	x_8
x_3	x_6	x_9

(1.1)

but consider still only row sums r_1, r_2, r_3 and column sums s_1, s_2, s_3 . This gives rise to the system

$$\begin{bmatrix} 1 & 1 & 1 & 0 & 0 & 0 & 0 & 0 & 0 \\ 0 & 0 & 0 & 1 & 1 & 1 & 0 & 0 & 0 \\ 0 & 0 & 0 & 0 & 0 & 0 & 1 & 1 & 1 \\ 1 & 0 & 0 & 1 & 0 & 0 & 1 & 0 & 0 \\ 0 & 1 & 0 & 0 & 1 & 0 & 0 & 1 & 0 \\ 0 & 0 & 1 & 0 & 0 & 1 & 0 & 0 & 1 \end{bmatrix} \begin{bmatrix} x_1 \\ x_2 \\ x_3 \\ x_4 \\ x_5 \\ x_6 \\ x_7 \\ x_8 \\ x_9 \end{bmatrix} = \begin{bmatrix} r_1 \\ r_2 \\ r_3 \\ s_1 \\ s_2 \\ s_3 \end{bmatrix} \quad (1.2)$$

This system has fewer equations than unknowns. Normally, such systems allow an infinity of solutions for any right hand side (RHS). In Section III.1, we show that in this case, solutions are possible only if $r_1 + r_2 + r_3 = s_1 + s_2 + s_3$, a natural restriction since both sides express the same quantity - the sum of all the unknowns. With this restriction satisfied, the same analysis shows further that we can choose for example the four entries x_5, x_6, x_8, x_9 arbitrarily and still satisfy (1.2).

Once the CT inversion problem has been formulated as linear system, such as (1.2), we see that we need at least as many equations as unknowns. If we have more equations than unknowns, the system becomes overdetermined. Then, there is typically no exact solution. However, least squares solutions can be found readily (cf. Section III.1), making the difference between LHS and RHS of a system, now shaped

$$\begin{bmatrix} \dots & \dots \\ \dots & \dots \\ \dots & \dots \\ \dots & \dots \\ \dots & \dots \\ \dots & \dots \end{bmatrix} \begin{bmatrix} \cdot \\ \cdot \\ \cdot \end{bmatrix} = \begin{bmatrix} \cdot \\ \cdot \\ \cdot \\ \cdot \\ \cdot \\ \cdot \end{bmatrix} \quad (1.3)$$

as small as possible. The way to get the additional equations is to send the probing X-rays in more directions through the object - i.e. not just horizontally and vertically. The entries in the coefficient matrix are now not only 0's or 1's (as in (1.2)), but instead real numbers which reflect how visible each box is to each ray. The coefficient matrix A will be quite sparse, but with a complicated sparsity structure, difficult to exploit well.

If we assume that for each of m angles, n rays are sent (to n receivers) through an object consisting of $n \times n$ 'blocks' (whose densities are to be determined), the structure of the system becomes as shown in Figure 1.3. Figure 1.4 illustrates how each of the m block-rows of A is formed. Each of these correspond to a certain angle of the rays. For any one of these angles, we consider sending a group of n rays through the grid on which the object is defined, and note how much the k^{th} ray 'interacts' with the i, j^{th} grid block (a measurement of how long distance the ray travels within each block as it cuts through it). This measure is then entered at the $(i + n \cdot j)^{\text{th}}$ location along the k^{th} row within the block-row of A that corresponding to the ray angle.

To use the *normal equation* approach (Section III.1), we form a linear $mn \times n^2$ system $Ax = b$ the square $n^2 \times n^2$ system

$$A^T Ax = A^T b .$$

Forming $A^T A$ will cost $O(mn^5)$ operations, $A^T b$ costs $O(mn^3)$; Cholesky decomposition of $A^T A$ into $L L^T$ will add another $O(n^6)$. The final step to get x through two back substitutions (using

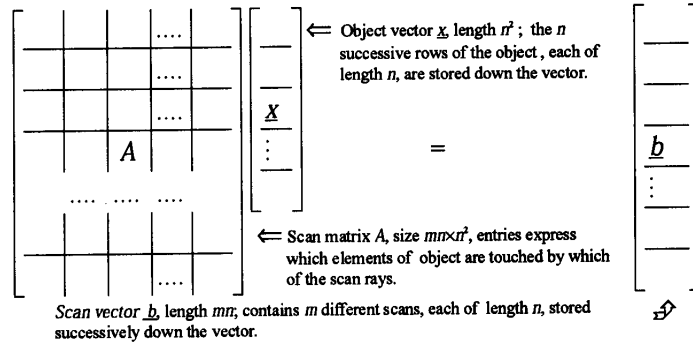


Figure 1.3: Structure of overdetermined linear system to solve for least-square method reconstruction.

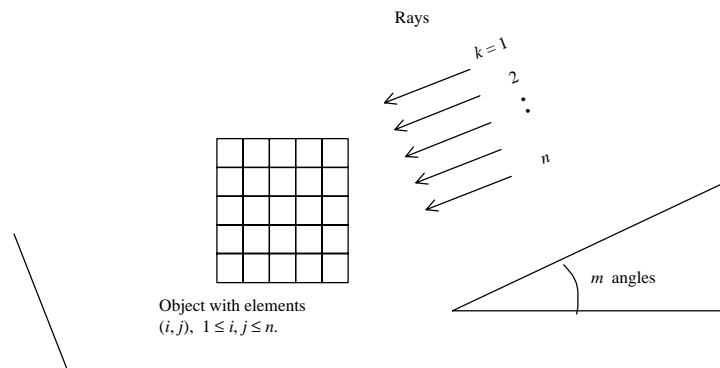


Figure 1.4: Illustration to the explanation for how the A -matrix entries are formed.

Comparisons of times for algorithms of different complexity on a system performing 10^8 floating point operations per second

Size $n \times n$ pixels	n^6 <small>(least squares)</small>	n^4 <small>(least squares)</small>	n^3 <small>(filtered BP)</small>	$n^2 \log n$ <small>(Fourier)</small>
$n = 100$	3 h	1 s	0.01 s	0.2 ms
$n = 1000$	320 y	3 h	10 s	0.03 s

Table 1.1: Comparison of computational efficiencies

L and L^T resp.) add a further $O(n^4)$ operations. Assuming m is just slightly larger than n , the total cost becomes $O(n^6)$ operations.

A very large saving can be realized by noting that the A -matrix is independent of the object we are studying - that will only affect the b - (and x -) vectors. The L -matrix can therefore be determined once and for all. Each image will then 'only' cost $O(n^4)$ operations. We will soon see that even this is not competitive - the next two methods, filtered back projection and Fourier method will cost only $O(n^3)$ and $O(n^2 \log n)$ respectively. Table 1.1 compares the computational time needed by the different approaches.

The least-squares approach requiring $O(n^6)$ operations was used by Hounsfield in his first successful experimental inversion. Already with a sample as coarse as 8×8 , the necessary computing took hours on EMI's then state-of-the-art ICL machine. The code `least_sq` in Section is a direct implementation of this approach. Figure 1.5 shows the result if our test object is scanned with 31 rays and 40 angles, followed by reconstruction with this method to a 31×31 grid. This level of resolution is too low for a good reconstruction, but we can still see a rough version of the ring and the central lettering.

Current medical imaging uses the filtered BP - method to be described next.

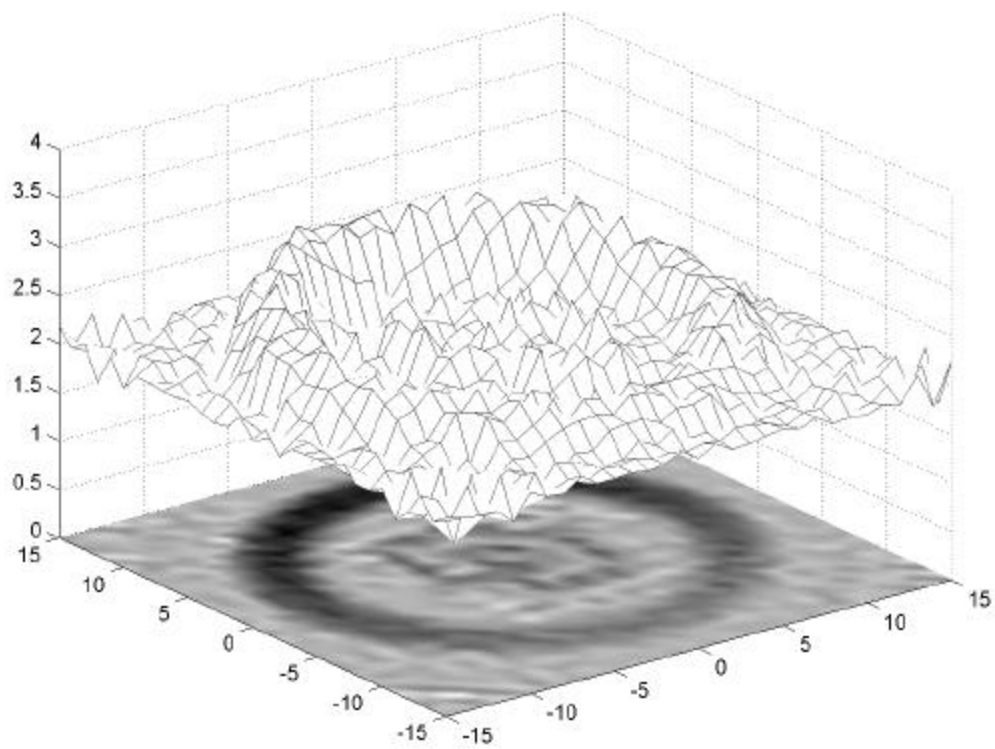


Figure 1.5: Reconstruction with the least squares method when the logo was scanned with 31 rays at 40 angles, followed by a reconstruction to a 30×30 grid.